Macromolecules

Article

pubs.acs.org/Macromolecules

The Roles of Blending and of Molecular Weight Distribution on Craze Initiation

Andrea Sánchez-Valencia,[†] Olga Smerdova,[†] Lian R. Hutchings,[‡] and Davide S. A. De Focatiis*[,†]

[†]Faculty of Engineering, University of Nottingham, Nottingham NG7 2RD, U.K.

[‡]Department of Chemistry, University of Durham, Durham DH1 3LE, U.K.

Supporting Information

ABSTRACT: Craze initiation stress was measured in three-point bending isochronal creep tests on a series of entangled bimodal blends of polystyrenes of narrow dispersity, on three polystyrenes of broad dispersity, and on four blends of polystyrenes of broad dispersity. Crazing stress was found to increase rapidly with small additions of the higher molar mass component, quickly reaching a plateau. A simple model based on the weighted addition of the crazing stress contributions of the individual weight fractions obtained from an established piecewise linear crazing law was able to predict the crazing stress accurately in the bimodal blends using a power law exponent of 2.59 (90% CI [1.75−17.34]). In broad dispersity systems, in particular where short unentangled chains dilute the polymer, it was found necessary to modify the model using dynamic tube dilution theory. Dilution leads to a change in the entanglement length and hence in the molar mass at which transitions to disentanglement and chain scission crazing occur. With the improved model, crazing stress could be predicted even for the broad dispersity polymers with wide and bimodal distributions. This represents an opportunity for the molecular design of polymers by blending to achieve improved resistance to craze initiation.

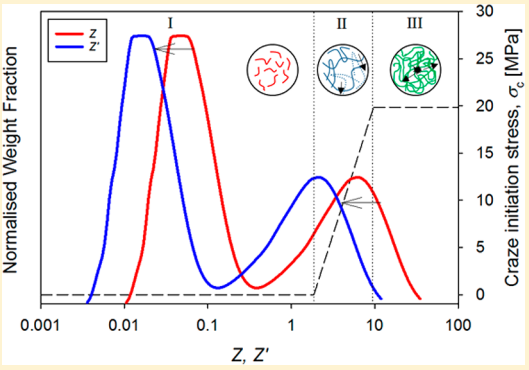

1. INTRODUCTION

Over the past few decades considerable effort has been devoted to understanding the role of microstructural characteristics on the macroscopic mechanical response of entangled polymers. Most of the early studies in this field employed polymers of broad molar mass distributions but differing molar mass averages to conclude that several properties of practical engineering interest such as tensile strength,[1,2] fracture toughness,[3] and fatigue life[4,5] can be linked to a measure of the molar mass distribution. In all of these cases, properties generally appear to depend on molar mass, up to a critical molar mass before saturating. Thus, much in the same way that the length of molecules is a critical parameter on the flow properties of polymer melts, it also plays an important role in the solid-state properties. Several authors have attempted to correlate polymer properties to specific averages of the molar mass distributions such as the number-average, $\bar{M}_n$, or the weight-average, $\bar{M}_w$,[6−8] and although this may be possible for polymers with similar distributions, different distributions can lead to the same averages but to vastly different properties.[9]

Homopolymer blending is a practical approach to tuning and improving properties of polymers to specific applications. The brittle-to-ductile transition of PS was observed to change as a function of molar mass and blending,[10] and it was shown that inherently brittle PS of narrow dispersity could be rendered tough, and hence more useful, by the addition of longer chains. In order to understand more precisely the role of molecular length, it is necessary to reduce the complexity of broad distributions in which not only does each molecule behave differently because of its own length but also because of the complex interchain interactions with other molecules, themselves of varying lengths. De Focatiis and co-workers recently carried out extensive studies of craze initiation,[11] orientation-induced birefringence,[12,13] and the constitutive response in the melt and solid states[14] of a range of narrow dispersity linear entangled polystyrenes (PS) and were able to link a number of properties more directly to chain length via fundamental concepts of polymer behavior such as Rouse times and reptation times. Although much progress has been made on the fundamental understanding of the role of chain length on polymer properties, many questions remain as to how distributions of lengths of polymer chains affect physical phenomena. In particular, when addressing properties of commercial polymers which have invariably broad distributions and are often blended, it is of considerable practical interest to address these fundamental questions within the context of dispersity.

Crazing, the formation of microscopic cracklike objects spanned by highly oriented polymer fibrils due to the application of stress over time, is one such phenomenon

Received: June 16, 2017
Revised: November 7, 2017
Published: November 20, 2017

DOI: 10.1021/acs.macromol.7b01289
Macromolecules 2017, 50, 9507−9514

where the role of chain length manifests itself very evidently. Early studies of crazing in PS identified that in order for a craze to form the molar mass M must be greater than a critical molar mass M_c, typically equal to two entanglement lengths.[15] Kramer and co-workers explored this further, with comprehensive studies on the effect of entanglements on crazing,[16] the stability of craze formation,[17] and the correlation between entanglements and craze microstructure.[18] One of the key contributions of Kramer and co-workers was the observation that in order for crazes to form a geometrically necessary entanglement loss of approximately 50% (at room temperature) was required[18−21] and that this might take place either by disentanglement or by chain scission. More recently, Ge et al.[22] used molecular dynamics to show that during craze formation about 1/3 of entanglement constraints change and that the associated chain dynamics occurs within the rheological tubes.

Synthesis of small quantities of narrow molar mass distributions ($\bar{M}_w/\bar{M}_n \leq 1.12$) and miniaturization of solid-state tests[23] enabled De Focatiis et al. to study craze initiation in PS over a wide range of molar mass, between 68 and 967 kDa.[11] The different crazing regimes suggested by Kramer could clearly be observed in polymers of different molar mass, and a simple model based on stress-accelerated disentanglement was able to account for the dependence of crazing stress on molar mass in the disentanglement regime consistently with other studies.[24] These developments provide a valuable starting point when addressing the issue of dispersity.

The objective of the present work is to explore further how molar mass distribution affects the phenomenon of craze initiation. Four bimodal blends made from three PS of narrow molecular weight distributions are investigated as well as three broad dispersity PS with different distributions and four melt-compounded blends of the broad dispersity PS. From the understanding obtained through the use of the bimodal blends, suggestions are made as to how dispersity might be accounted for in more general, broad distributions and compared to experimental measurements. The methods proposed offer new insight into the role of molecular weight distribution on solid-state properties and should be of direct practical interest to polymer designers looking to alter properties by blending.

2. MATERIALS AND METHODS

2.1. Materials. The narrow dispersity linear atactic PS materials used in this study were synthesized through living anionic polymerization to produce three samples of low, medium, and high molar mass. These were blended by solution blending, with tetrahydrofuran (THF) as the solvent. The constituent materials were codissolved in THF to give a 5 wt % solution. The blend solutions were stirred for 1.5 h prior to precipitation into an excess of methanol (THF:methanol = 1:6). The polymers were then recovered by vacuum filtration and dried at 50 °C in a vacuum oven to constant mass.

The broad dispersity PS materials were obtained from the Dow Chemical Company and from Sigma-Aldrich in the form of granules. Four further blends of broader dispersity were produced by melt-mixing, combining components BX and BY at mass ratios of 5:95, 10:90, 20:80, and 50:50. The melt-mixing process was carried out using a twin-screw recirculating extruder HAAKE Mini-Lab II Rheomex CTW 5 fitted with corotating conical screws. The mixing was carried out at 200 °C at 50 rpm for 15 min.

Molar mass distributions were measured using size exclusion chromatography (SEC) using an Agilent system with a Wyatt Dawn multiangle light scattering detector using tetrahydrofuran (THF) as the eluent. Averages of the molar mass distributions were computed using Matlab. Molar mass distributions for melt-mixed blends were obtained by calculation from their constituents. Further details of the polymers and averages of the distributions are reported in Table 1, and the normalized molar mass distributions are presented in Figure 1.

Table 1. Compositions (by Weight) and Molar Mass Averages Obtained by SEC for the Polystyrene Materials Used in This Study[a]

code	molar mass distribution	type and composition	$\bar{M}_n$ (kDa)	$\bar{M}_w$ (kDa)	$Đ^b$
BF	narrow	low M	86.1	93.4	1.08
BG		medium M	251.3	269.9	1.07
BH		high M	470.0	540.3	1.15
BI	bimodal blends	90% BF, 10% BG	93.2	117.8	1.26
BJ		80% BF, 20% BG	96.6	133.9	1.38
BK		50% BF, 50% BG	134.0	192.1	1.43
BL		80% BF, 20% BH	110.8	191.2	1.72
R	broad	Dow GP-PS680E	85.2	221.7	2.60
BX		Sigma-Aldrich 35K	1.4	47.8	32.91
BY		Sigma-Aldrich 350K	158.6	339.2	2.14
CA	broad blends	95% BX, 5% BY	1.5	62.3	40.75
CB		90% BX, 10% BY	1.6	76.9	47.7
CC		80% BX, 20% BY	1.8	106.0	58.5
CD		50% BX, 50% BY	2.9	193.5	67.1

[a]For materials CA−CD the averages were computed from SEC data based on the components. [b]Dispersity.

In order to interpret the chain lengths in terms of the number of entanglements, linear viscoelastic rheological measurements on materials BF, BG, and BH were fitted to the theory of Likhtman and McLeish[6] to give M_e = 15.9 kDa, a value consistent with the range of 12.9−16 kDa found in recent literature.[14,25,26] Further details are provided in the Supporting Information.

2.2. Production of Solid Specimens. Because of the limited quantities of materials available, a technique for near net shape production of miniature parallelepipedic bars was employed to minimize material waste.[23] Discs of 0.5 mm in thickness and 25 mm in diameter were produced by hot compression molding following a standard procedure.[27] A steel cavity mold enclosed by upper and lower steel plates was placed in a hand-operated hydraulic press with heated platens at 170 °C. Fresh sheets of disposable aluminum foil were lightly coated with PTFE release spray and positioned between the steel plates and the cavity mold to provide a repeatable surface roughness. Each material was allowed to heat for a period of 5 min, after which time pressure was cycled to dislodge any trapped air bubbles. The material was held for a further 10 min at 170 °C to allow full relaxation and produce optically isotropic materials. After this time, the material was cooled at a rate of ca. 15 °C min^{-1} through to a temperature below the glass transition. The discs were then carefully removed from the mold. Miniature beam specimens with dimensions of 7 mm × 2 mm × 0.5 mm were produced by cutting using a jig with parallel single beveled blades.[23] The beam specimens were immersed in diethylene glycol (DEG), a mild crazing agent, for a minimum of 24 h prior to creep testing to induce crazes.

2.3. Miniature Creep Crazing Experiments. The miniature beam specimens were subjected to isochronal three-point bending creep with the aid of custom-made test rigs.[23] The use and validation of this technique have been described in previous publications,[11,12] and only a brief account is given here. The test consists in applying a creep load to miniature beam specimens subjected to three-point bending in order to promote craze formation in an approximately triangular region where the (tensile) stress is sufficient to initiate crazes. The load was applied centrally for a fixed creep time of t_c = 300 s. The creep test was carried out in the presence of DEG. When a sufficient creep load was applied, stable crazes formed perpendicular to the beam axis. After unloading, the specimen was wiped to remove excess DEG and placed with the beam axis at a small-angle to the horizontal under a low-power optical microscope, such that transmitted light incident to the beam surface at double the angle was reflected by the crazes along the

DOI: 10.1021/acs.macromol.7b01289
Macromolecules 2017, 50, 9507−9514

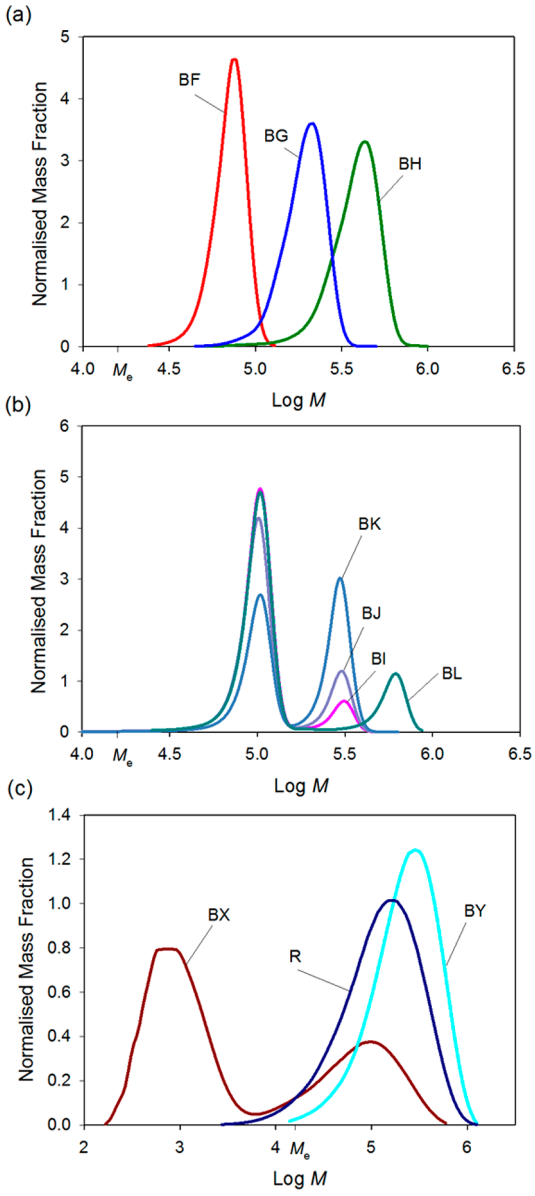

Figure 1. Narrow dispersity (a), bimodal blends (b), and broad dispersity (c) molar mass distributions of materials obtained from SEC data.

optic axis of the microscope, thus making the crazes visible. Within 1 h of crazing, five measurements of the length of the crazed region were made across the width of the specimen in order to obtain a mean crazed length, l_c. The craze initiation stress, σ_c, required for crazes at the edge of the region to form just enough to become visible, was then computed using elementary beam theory as[23]

$$\sigma_c = \frac{3P(l - l_c)}{2bd^2} \quad (1)$$

where P is the applied load, l = 5 mm is the support spacing, and b and d represent the width and thickness of the specimen, measured using a micrometer. The crazing stress is not itself dependent on the magnitude of the creep load (since bigger loads cause longer crazed regions) but has to be sufficient to initiate crazes and small enough for specimens not to fracture in the creep time.

3. RESULTS

3.1. Narrow Distributions. The craze initiation stresses recorded for the narrow distribution materials are presented in Table 2.

Table 2. Craze Initiation Stress of Narrow Distribution Materials at t_c = 300 s

code	exptl σ_c [MPa]	no. of tests
BF	16.0 ± 0.1	2
BG	22.2 ± 1.3	11
BH	23.6 ± 1.1	9

A minimum of nine specimens of each material were crazed, with the exception of material BF, for which it was challenging to form a crazed region without fracturing the specimen and for which the average reported here is obtained only from two specimens. Similar difficulties in forming stable crazes in low molar mass PS were also reported by other authors.[17,28] Results are given as mean ±2 standard errors.

3.2. Bimodal Blends of Narrow Distributions. Figure 2 shows measurements of σ_c carried out on the PS bimodal

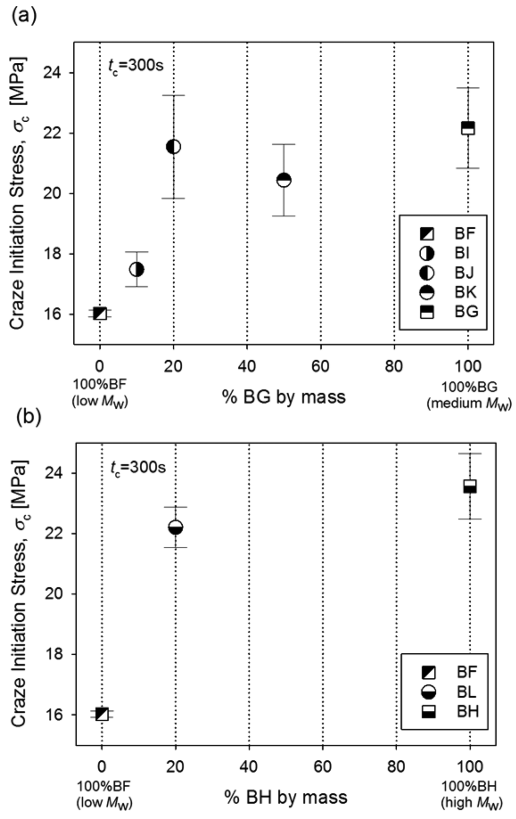

Figure 2. Craze initiation stress as a function of blend composition for (a) blends of materials BF and BG and (b) blends of materials BF and BH, all for t_c = 300 s.

blends as a function of the blend ratio. Figure 2a shows blends of components BF and BG, and Figure 2b shows blends of BF and BH. A minimum of six specimens of each blend material were crazed.

The results in Figure 2 clearly reveal that as little as 20% of a higher molar mass component in a lower molar mass matrix leads to a noticeable increase in σ_c. Craze formation was also

DOI: 10.1021/acs.macromol.7b01289
Macromolecules 2017, 50, 9507−9514

observed to become more stable with the addition of a higher molar mass material, and larger creep loads could be used to craze a longer region. Also apparent is that the value of σ_c rapidly reaches a plateau once ~20% of the higher molar mass components is added.

3.3. Broad Distributions. Measurements of σ_c recorded for broad distribution materials R, BX, and BY are presented in Table 3.

Table 3. Craze Initiation Stress for Broad Distribution Materials at t_c = 300 s

code	exptl σ_c [MPa]	no. of tests
R	22.6 ± 0.9	27
R[a]	19.5 ± 0.7	100
BX[b]	≤2.4	>10
BY	23.3 ± 1.7	6

[a]Data from De Focatiis et al.[11] [b]Estimate based on one successful test due to difficulties in producing stable crazes in brittle specimens.

It proved challenging to form stable crazes in material BX. Specimen preparation was exceptionally difficult due to its brittleness and multiple specimens fractured during the creep load. One specimen crazed during loading, but fractured during transport to the optical inspection, and appeared to have a single craze in the middle, from which the crazing stress of ≤2.4 MPa is estimated.

4. DISCUSSION

4.1. Role of Molar Mass in Narrow Distributions. It is apparent from Table 2 that in the narrow distribution polymers tested here the higher the molar mass, the higher the value of σ_c. This is consistent with earlier, more extensive measurements of crazing in narrow distribution PS.[11] A direct comparison of the data from this paper with published data[11] is shown in Figure 3. A small correction was applied to the data from ref 11 to account for more precise measurements of the span.[a]

Material BF lies in the middle of region II, previously identified with a strong molar mass dependence and suggested to be crazing by molecular disentanglement. A model of the form $\sigma_c = a_0 + a_1 \ln M$ was previously proposed to account for this dependence up to ~150 kDa.[11] Materials BG and BH instead lie within region III, where σ_c becomes independent of molar mass such that $\sigma_c = \sigma_\infty$ and associated with a crazing mechanism by chain scission. Region I is where $M < 2M_e$, and the polymer is insufficiently entangled to form a network.[2,15,17,20]

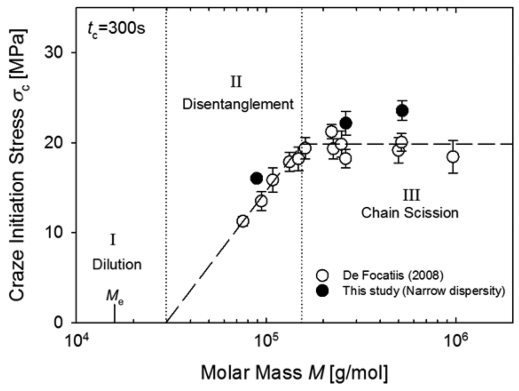

Figure 3. Isochronal measurements of craze initiation stress (t_c = 300 s) as a function of molar mass M for narrow distribution linear PS; data from this study (filled symbols) and from De Focatiis et al.[11] (hollow symbols). Data from ref 11 were corrected for the actual support spacing by consideration of the radii of curvature of the supports (see footnote *a*). The disentanglement and chain scission regimes are visible.

Despite a small systematic difference in the absolute measured values of σ_c, attributed to differences in the optical setup used to detect nascent crazes, the data sets are consistent. Further analysis of the creep time dependence of craze initiation (provided in the Supporting Information) also confirmed that samples BG and BH are of a length sufficient to exhibit molar mass independent craze behavior, associated with chain scission.

4.2. Bimodal Blends. A rise in σ_c with increasing higher molar mass component was noted in both blends. It is not immediately apparent how the presence of relatively small quantities of higher molar mass components leads to quite noticeable increases in σ_c, but it is reasonable that σ_c^{blend} could be determined by a weighted addition of the measured σ_c^{mono} values for the components $\sigma_c^{blend} = \sum_M \phi(M)\sigma_c^{mono}(M)$, where $\phi(M)$ are weighting factors, themselves possibly depending on the molar mass in question. A possible generalized description of the weighting factor is given by

$$\phi_\theta(M) = \frac{n(M)M^{\theta-1}}{\sum_M n(M)M^{\theta-1}} \tag{2}$$

where $n(M)$ is the number of moles of species M and θ is an exponent. In this particular form, the traditional molar mass averages are simply given as

$$\bar{M}_\theta = \frac{\sum_M n(M)M^\theta}{\sum_M n(M)M^{\theta-1}} = \sum_M \phi_\theta(M)M \tag{3}$$

and here one may recover $\bar{M}_n$, the number-average molar mass, for θ = 1, and $\bar{M}_w$, the weight-average molar mass, for θ = 2. Thus, one may write

$$\sigma_{c,\theta}^{blend} = \sum_M \phi_\theta(M)\sigma_c(M) \tag{4}$$

as a θ-prediction of molar mass based on a particular weighting of the distribution.

This is not an entirely new concept, and other studies have explored the correlation of physical properties with molar mass averages. In their analysis of tensile properties in polystyrene, Bersted and Anderson[29] were successful at linking tensile strength to a modified average of the distribution in relatively narrow dispersity polystyrene distributions and could accurately predict tensile property data.

In order to determine the value of θ consistent with the experimental measurements of crazing stress, the measured distributions of both the monodisperse BF, BG, and BH and of the bimodal blends BI, BJ, BK, and BL were fitted to the crazing model of eq 4 using a least-squares algorithm, and a Monte Carlo approach (n = 1000) was used to obtain a confidence interval (CI) on its value.[30] A value of θ = 2.59 (90% CI [1.75, 17.34]) was identified from the analysis. Figure 4 shows a comparison of predicted and measured crazing stresses for the bimodal blends.

It should be pointed out that the predictor for crazing stress with a θ value of 2.59 is not equivalent to simply working out the 2.59th order molar mass average since it is still dependent

DOI: 10.1021/acs.macromol.7b01289
Macromolecules 2017, 50, 9507−9514

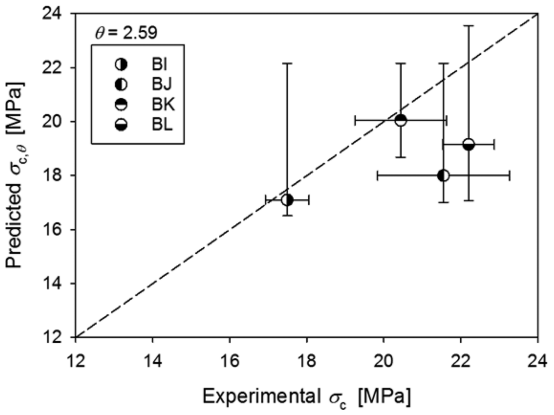

Figure 4. Comparison of model predictions and experimental measurements of craze initiation stress in bimodal blends BI, BJ, BK, and BL, using θ = 2.59 (90% CI [1.75, 17.34]).

on the values of crazing stress attributed to the specific molar mass of each component. Since the crazing stress follows a piecewise linear function of the logarithm of molar mass, this knowledge is required in order to evaluate the prediction.

The value of 2.59 may itself be significant since it suggests that the crazing mechanism is linked to a quantity that scales with a higher power of molar mass. The mechanism for disentanglement crazing proposed by De Focatiis et al.[11] was linked to the Rouse time, a quantity that scales with the square of molar mass, and it is known that polymeric reptation times scale with a power of 3−3.4 of molar mass,[26,31] so the data here suggest that the cooperative effect of different length scales for crazing in a bimodal blend is related to time scales associated with tube constraints.[22] Unfortunately, the large statistical uncertainty on the value of θ precludes a more precise determination.

4.3. Application to Generic Dispersity. In a generic broad distribution, the molar mass fractions could span across all three crazing regimes.[11] Hence, the contribution to crazing of every molar mass fraction, $\phi_\theta(M)$, is needed based on the corresponding crazing mechanism of the molar mass in question: region I, dilution; region II, disentanglement; and region III, chain scission. Starting with the assumption that unentangled chains do not contribute to resisting craze initiation, the piecewise linear approach is defined by

$$\sigma_c(M) = \begin{cases} 0, & M < M_c \\ \sigma_\infty \dfrac{M - M_c}{M_\infty - M_c}, & M_c < M < M_\infty \\ \sigma_\infty, & M > M_\infty \end{cases} \quad (5)$$

where σ_∞ is the chain scission crazing stress saturation value at M_∞, and M_c represents the critical molar mass limit at which the entanglement network forms and crazing by disentanglement occurs. Using constants derived from the corrected literature data[11] of M_c = 39.6 kDa, M_∞ = 154.2 kDa, and σ_∞ = 19.85 MPa, a Matlab code was written to compute the crazing stress for distributions R, BX, and BY using a θ value of 2.59, and the results are given in Table 4.

The application of the model produces reasonable predictions of crazing stress for materials R and BY but overpredicts the crazing stress for material BX by a factor of 6 (Table 4, without DTD). The molar mass distributions, shown in Figure 1c, for materials R and BY lie predominantly in the disentanglement and chain scission regimes, while that for material BX shows a distinct bimodal distribution that spans across all three regimes, with a significant fraction in the unentangled dilution region. This suggests that the current model is incorrectly dealing with the contribution of the unentangled fraction that is so dominant in polymer BX.

Table 4. Experimentally Measured CIS and Theory Predictions Using θ = 2.59 with a 90% Confidence Interval of [1.75−17.34] for Broad Dispersity Materials

		predicted σ_c [MPa]		
code	exptl σ_c [MPa]	without DTD	with DTD	concn, c
R[a]	19.5 ± 0.7	17.9 [14.0, 19.8]	17.6 [13.8, 19.5]	0.982
BX[b]	≤2.4	13.7 [1.7, 19.8]	4.7 [0.6, 6.8]	0.341
BY	23.3 ± 1.7	19.1 [16.9, 19.8]	19.0 [16.8, 19.7]	0.993

[a]Data from De Focatiis et al.[11] [b]Estimate based on one successful test due to difficulties in producing stable crazes in brittle specimens.

4.4. Implementing a Dilution Correction. Marrucci suggested the concept of dynamic tube dilation (DTD)[32] to explain how constraint release mechanisms in polymer molecules are modified by a change in the entanglement tube diameter. When a polymer system is in the presence of a diluent, the tube circumference expands as the entangled polymer concentration is reduced. This reduction also affects the overall mobility of the longer chains as the number of entanglements decreases and the molar mass between two entanglements, M_e, becomes larger. Several rheological studies[33−35] have been able to predict the viscoelastic response of blends and solutions by acknowledging the DTD effect and fine-tuning the value of the dynamic dilution exponent, α. Recently, a modified expression for M_e accounting for this behavior in diluted monodisperse PS systems was proposed by Shahid[36]

$$M_e = \frac{M_{e,0}}{(c\phi)^\alpha} \quad (6)$$

where c is the polymer concentration, $M_{e,0}$ is the entanglement molar mass of an undiluted system, and ϕ is the fraction of unrelaxed polymer.

In applying Marucci's and Shahid's ideas to our crazing model, we treat the unentangled fraction of short chains as a diluent and evaluate the entangled concentration from

$$c = \sum_{M_e}^{\infty} w(M) \quad (7)$$

using a value of $M_{e,0}$ = 15.9 kDa, as obtained from oscillatory rheological data in the narrow dispersity PS materials BF, BG, and BH. Concentrations of entangled chains in the broad distributions studied are evaluated and shown in Table 4. Here only polymer BX has a concentration significantly lower than unity.

Taking α = 1, and considering the remaining entangled molecules in their unrelaxed state, the effective molar mass between entanglements is simply given by $M_e = M_{e,0}/c$. Applying this to the definition of the number of entanglements Z, traditionally given simply by $M/M_{e,0}$,[26] gives a modified number of entanglements Z' in a diluted system as

$$Z' = \frac{cM}{M_{e,0}} \quad (8)$$

DOI: 10.1021/acs.macromol.7b01289
Macromolecules 2017, 50, 9507−9514

Hence, the presence of unentangled short chains decreases the number of entanglements in the system and shifts the balance of the mechanisms of crazing. In Figure 5, the molar mass

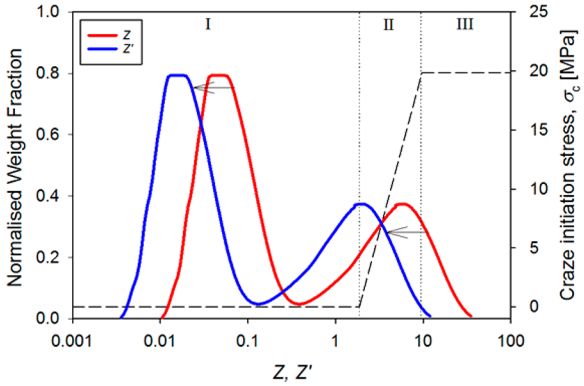

Figure 5. SEC distribution normalized with respect to M_e to give the number of entanglements Z or the effective number of entanglements Z' for material BX (left abscissa); piecewise linear crazing stress function illustrating the different crazing regimes, I (dilution), II (disentanglement), and III (chain scission). The contribution of the different parts of the distribution to craze initiation can be observed.

distribution of material BX is shown as a function of both the nominal number of entanglements Z and the effective number of entanglements Z' including dilution. The result of considering the effective number of entanglements is to shift the distribution to the left. Also shown on the same plot is the piecewise linear crazing model, now expressed in terms of the number of entanglements rather than of molar mass.

If we now interpret the proposed model in terms of the effective number of entanglements, the piecewise model is now expressed as

$$\sigma_c(Z') = \begin{cases} 0, & Z' < Z'_c \\ \sigma_\infty \dfrac{Z' - Z'_c}{Z'_\infty - Z'_c}, & Z'_c < Z' < Z'_\infty \\ \sigma_\infty, & Z' > Z'_\infty \end{cases} \quad (9)$$

with $Z'_c = cM_c/M_e$ and $Z'_\infty = cM_\infty/M_e$. Hence, the crazing stress of a given component of the distribution shifts to a lower molar mass equivalent, depending on the magnitude of c. The new predictions of crazing stress corrected for dilution are therefore given by

$$\sigma_{c,\theta}^{\text{blend}} = \sum_{Z'} \phi_\theta(Z')\sigma_c(Z') \quad (10)$$

and are also shown in Table 4.

The effect of this correction is to change the prediction of crazing stress for material BX from 13.7 to 4.7 MPa, much closer to the experimentally recorded value of 2.4 MPa. Only very minor changes to the predictions for polymers R and BY take place since the dilution is very slight. This more detailed interpretation of the effects of the different length scales within a blend on crazing is not only physically more realistic but also able to produce relatively accurate predictions of crazing stress in all the analyzed materials.

To further test the applicability of model and of the dilution correction, it was applied on numerically evaluated molar mass distributions for the four further melt-mixed blends of components BX and BY, such as might be carried out in industry for the purpose of selecting a blend. The values of the experimentally measured σ_c are compared to theory predictions in Table 5, using θ = 2.59, both with and without DTD. The predictions with DTD including 90% confidence intervals are also compared to experimentally measured values in Figure 6.

Table 5. Experimentally Measured CIS and Theory Predictions Using θ = 2.59 with a 90% Confidence Interval of [1.75−17.34] for Blends of Broad Dispersity Materials

		predicted σ_c [MPa]		
code	exptl σ_c [MPa]	without DTD	with DTD	concn, c
CA[a]	~1.9	14.8 [1.9, 19.8]	5.5 [0.7, 7.4]	0.373
CB[a]	~3.0	15.5 [2.2, 19.8]	6.3 [0.9, 8.1]	0.406
CC	6.1 ± 1.68	16.6 [2.9, 19.8]	7.8 [1.3, 9.4]	0.471
CD	10.8 ± 1.86	18.1 [5.6, 19.8]	12.1 [3.7, 13.2]	0.667

[a]Experimental value obtained on a single successful test due to difficulties in producing stable crazes in brittle specimens.

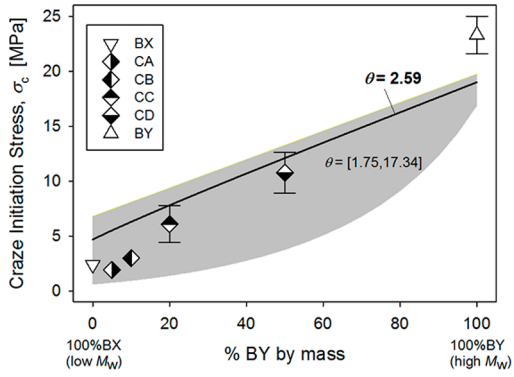

Figure 6. Experimentally measured craze initiation stress (symbols) as a function of blend composition for blends of materials BX and BY, compared with theory predictions including the effects of DTD, for t_c = 300 s, using θ = 2.59 (solid line), with 90% confidence intervals (shaded region).

5. CONCLUSIONS

This work has investigated the relationship between craze initiation and molar mass distribution in a series of bimodal blends of narrow distributions of polystyrene, a second series of broad distribution polystyrenes, and a third series of blends of broad distribution polystyrenes. Isochronal experiments carried out in three-point bending creep showed that in both the blends and the broad distributions systems the crazing stress was found to be heavily dominated by the presence of a high molar mass component. A simple model was proposed that sums the weighted crazing stress contributions of the mass fractions based on a piecewise linear crazing law. With this model, crazing stresses could be accurately predicted in the bimodal blends using a power law exponent of 2.59. The initial model was less successful when trying to predict crazing stress of one broad distribution material, mainly due to a substantial fraction of unentangled polymer chains. Employing concepts from dynamic tube dilution theory, the model was modified to instead base the prediction on the basis of the change in entanglement length caused by the short chains. This improved model was used to more accurately predict the crazing stress of the aforementioned broad dispersity polymer. To further validate the model, craze initiation was measured on four melt-mixed blends of broad dispersity polystyrenes. The model

DOI: 10.1021/acs.macromol.7b01289
Macromolecules 2017, 50, 9507−9514

including DTD effects was able to successfully predict the crazing stress in all blends with a significant fraction of unentangled chains. The model, and the concepts underpinning it, should be useful to polymer designers looking to find ways of increasing resistance to craze initiation without adversely affecting other aspects of the polymer behavior, such as its rheology.

■ ASSOCIATED CONTENT

Supporting Information

The Supporting Information is available free of charge on the ACS Publications website at DOI: 10.1021/acs.macromol.7b01289.

Figures S1 and S2 (PDF)

■ AUTHOR INFORMATION

Corresponding Author

*E-mail davide.defocatiis@nottingham.ac.uk (D.S.A.D.F.).

ORCID

Davide S. A. De Focatiis: 0000-0002-2655-0508

Present Address

O.S.: Département Physique et Mécanique des Matériaux, Institut Pprime, CNRS, ISAE-ENSMA, Université de Poitiers, F-86962 Futuroscope Chasseneuil, France.

Notes

The authors declare no competing financial interest.

■ ACKNOWLEDGMENTS

This work was supported by the Engineering and Physical Sciences Research Council [grant number EP/J007978/1]. The authors wish to acknowledge the contribution of Dr. Alex Ilchev for the analysis and discussion of the SEC data, and Mrs Magdalena Patel for the support in the preparation of the melt-mixed specimens.

■ ADDITIONAL NOTE

[a]An error was identified in the determination of the crazing stress measurements in ref 11. The measurements failed to take into account the increased span between the supports caused by a small curvature at the support edges. The supports of the original rig and of the one used in this study were measured accurately using optical microscopy. The radii of the left (LHS) and right (RHS) supports of the original fixture are 284 ± 13 and 250 ± 8 μm and of the fixture used in this study are 27 ± 2 and 102 ± 9 μm. A correction to the measured crazing stress values reported in ref 11 was then determined using $\sigma_c = \sigma_c^{old}(l_u - l_c)/(l_n - l_c)$, where l_u is the uncorrected support spacing and l_n the new corrected support spacing.

■ REFERENCES

(1) Merz, E. H.; Nielsen, L. E.; Buchdahl, R. Influence of Molecular Weight on the Properties of Polystyrene. *Ind. Eng. Chem.* **1951**, *43* (6), 1396−1401.

(2) Sauer, J. A.; Hara, M. Effect of Molecular Variables on Crazing and Fatigue of Polymers. *Adv. Polym. Sci.* **1990**, *91/92*, 69−118.

(3) Nunes, R. W.; Martin, J. R.; Johnson, J. F. Influence of Molecular Weight and Molecular Weight Distribution on Mechanical Properties of Polymers. *Polym. Eng. Sci.* **1982**, *22* (4), 205−228.

(4) Foden, E.; Morrow, D. R.; Sauer, J. A. The Effect of Molecular Weight on the Fatigue Behavior of Polystyrene. *J. Appl. Polym. Sci.* **1972**, *16*, 519−526.

(5) Sauer, J. A.; Foden, E.; Morrow, D. R. Influence of Molecular Weight on Fatigue Behavior of Polyethylene and Polystyrene. *Polym. Eng. Sci.* **1977**, *17* (4), 246−250.

(6) Likhtman, A. E.; McLeish, T. C. B. Quantitative Theory for Linear Dynamics of Linear Entangled Polymers. *Macromolecules* **2002**, *35*, 6332−6343.

(7) Cazes, J. *A Question of Molecular Weight*; Waters Associates, Inc., 34 Maple St., Mildford, MA 01757.

(8) Meijer, H. E. H.; Govaert, L. E. Mechanical performance of polymers systems: The relation between structure and properties. *Prog. Polym. Sci.* **2005**, *30*, 915−938.

(9) Huang, Q.; Mednova, O.; Rasmussen, H. K.; Alvarez, N. J.; Skov, A. L.; Almdal, K.; Hassager, O. Concentrated polymer solutions are different from melts: role of entanglement molecular weight. *Macromolecules* **2013**, *46* (12), 5026−5035.

(10) Liu, J.; Lin, P.; Cheng, S.; Wang, W.; Mays, J. W.; Wang, S.-Q. Polystyrene Glass under Compression: Ductile and Brittle Responses. *ACS Macro Lett.* **2015**, *4*, 1072−1076.

(11) De Focatiis, D. S. A.; Buckley, C. P.; Hutchings, L. R. Roles of Chain Length, Chain Architecture, and Time in the Initiation of Visible Crazes in Polysyterene. *Macromolecules* **2008**, *41*, 4484−4491.

(12) De Focatiis, D. S. A.; Buckley, C. P. Craze initiation in glassy polymers: Quantifying the influence of molecular orientation. *Polymer* **2011**, *52* (18), 4045−4053.

(13) De Focatiis, D. S. A.; Buckley, C. P. Prediction of frozen-in birefringence in oriented glassy polymers using a molecularly aware constitutive model allowing for finite molecular extensibility. *Macromolecules* **2011**, *44*, 3085−3095.

(14) De Focatiis, D. S. A.; Embery, J.; Buckley, C. P. Large Deformations in Oriented Polymer Glasses: Experimental Study and a New Glass-Melt Constitutive Model. *J. Polym. Sci., Part B: Polym. Phys.* **2010**, *48*, 1449−1463.

(15) Fellers, J. F.; Kee, B. F. Crazing Studies of Polystyrene. I. A new Phenomenological Observation. *J. Appl. Polym. Sci.* **1974**, *18*, 2355−2365.

(16) Donald, A. M.; Kramer, E. J. Effect of Molecular Entanglements on Craze Microstructure in Glassy Polymers. *J. Polym. Sci., Polym. Phys. Ed.* **1982**, *20*, 899−909.

(17) Yang, A. C.-M.; Kramer, E. J.; Kuo, C. C.; Phoenix, S. L. Craze Fibril Stability and Breakdown in Polystyrene. *Macromolecules* **1986**, *19*, 2010−2019.

(18) Berger, L. L. Relationship between Craze Microstructure and Molecular Entanglements in Glassy Polymers. 1. *Macromolecules* **1989**, *22*, 3162−3167.

(19) Berger, L. L.; Kramer, E. J. Chain Disentanglement during High-Temperature Crazing of Polystyrene. *Macromolecules* **1987**, *20*, 1980−1985.

(20) Kramer, E. J. Microscopic and molecular fundamentals of crazing. *Adv. Polym. Sci.* **1983**, *52-53*, 1−56.

(21) Bueche, F. Molecular basis for the mullins effect. *J. Appl. Polym. Sci.* **1960**, *4* (10), 107−114.

(22) Ge, T.; Tzoumanekas, C.; Anogiannakis, S. D.; Hoy, R. S.; Robbins, M. O. Entanglements in Glassy Polymer Crazing: Cross-Links or Tubes? *Macromolecules* **2017**, *50* (1), 459−471.

(23) De Focatiis, D. S. A.; Buckley, C. P. Determination of craze initiation stress in very small polymer specimens. *Polym. Test.* **2008**, *27* (2), 136−145.

(24) Han, H. Z. Y.; McLeish, T. C. B.; Duckett, R. A.; Ward, N. J.; Johnson, A. F.; Donald, A. M.; Butler, M. Experimental and Theoretical Studies of the Molecular Motions in Polymer Crazing. 1. Tube Model. *Macromolecules* **1998**, *31*, 1348−1357.

(25) Carrot, C.; Majeste, J.-C. A modified tube dilation theory for the relaxation of entangled linear polymer melts. *J. Non-Newtonian Fluid Mech.* **2005**, *129*, 98−105.

(26) van Ruymbeke, E.; Liu, C.-Y.; Bailly, C. Quantitative tube Model Predictions for the Linear Viscoelasticity of Linear Polymers. *Rheol. Rev.* **2007**, 53−134.

(27) De Focatiis, D. S. A. Tooling for near net-shape compression moulding of polymer specimens. *Polym. Test.* **2012**, *31* (4), 550−556.

DOI: 10.1021/acs.macromol.7b01289
Macromolecules 2017, 50, 9507−9514

(28) Donald, A. M.; Kramer, E. J. Craze microstructure and molecular entanglements in polystyrene-poly(phenylene oxide) blends. *Polymer* **1982**, *23*, 461−465.
(29) Bersted, B. H.; Anderson, T. G. Influence of Molecular Weight and Molecular Weight Distribution on the Tensile Properties of Amorphous Polymer. *J. Appl. Polym. Sci.* **1990**, *39*, 499−514.
(30) Berendsen, H. J. C. *A Student's Guide to Data and Error Analysis*; Cambridge University Press: 2011.
(31) Doi, M. Explanation for the 3.4-power law for viscosity of polymeric liquids on the basis of the tube model. *J. Polym. Sci., Polym. Phys. Ed.* **1983**, *21* (5), 667−684.
(32) Marrucci, G. Relaxation by reptation and tube enlargement: A model for polydisperse polymers. *J. Polym. Sci., Polym. Phys. Ed.* **1985**, *23*, 159−177.
(33) Colby, R. H.; Rubinstein, M. Two-parameter scaling for polymers in θ solvents. *Macromolecules* **1990**, *23*, 2753−2757.
(34) van Ruymbeke, E.; Masubuchi, Y.; Watanabe, H. Effective value of the dynamic dilution exponent in bidisperse linear polymers: from 1 to 4/3. *Macromolecules* **2012**, *45*, 2085−2098.
(35) van Ruymbeke, E.; Shchetnikava, V.; Matsumiya, Y.; Watanabe, H. Dynamic Dilution Effect in Binary Blends of Linear Polymers with Well-Separated Molecular Weights. *Macromolecules* **2014**, *47*, 7653−7665.
(36) Shahid, T.; Huang, Q.; Oosterlinck, F.; Clasen, C.; van Ruymbeke, E. *Soft Matter* **2017**, *13*, 269.

DOI: 10.1021/acs.macromol.7b01289
Macromolecules 2017, 50, 9507−9514